Appl Phys A (2008) 92: 821–829
DOI 10.1007/s00339-008-4582-3

Applied Physics A
Materials Science & Processing

Generation of surface features in films deposited by matrix-assisted pulsed laser evaporation: the effects of the stress confinement and droplet landing velocity

Aaron Sellinger · Elodie Leveugle · James M. Fitz-Gerald · Leonid V. Zhigilei

Received: 12 October 2007 / Accepted: 4 March 2008 / Published online: 22 May 2008

Abstract Coarse-grained molecular dynamics simulations are applied to investigate the origins of the surface features observed in films deposited by the Matrix-Assisted Pulsed Laser Evaporation (MAPLE) technique. The formation of transient balloon-like structures with a polymer-rich surface layer enclosing matrix vapor, observed in earlier simulations of slow heating of polymer-matrix droplets, has been explored in this work at higher rates of thermal energy deposition. Tensile stresses generated in the regime of partial stress confinement are found to induce an internal boiling in the overheated droplets and associated generation of "molecular balloons" at thermal energy densities at which no homogeneous boiling takes place without the assistance of tensile stresses. Simulations of the dynamic processes occurring upon the collision of a polymer-matrix droplet with a substrate provide the molecular-level pictures of the droplet impact phenomenon and reveal the connections between the droplet landing velocity and the shapes of the polymer features observed in scanning electron microscopy images of films deposited in MAPLE experiments. The distinct types of surface features observed in MAPLE experiments, namely, wrinkled "deflated balloons," localized arrangements of interconnected polymer filaments, and elongated "nanofibers," are shown to emerge from different scenarios of droplet landing and/or disintegration observed in the simulations.

PACS 81.15.Fg · 02.70.Ns · 61.80.Az · 64.60.Ht · 83.80.Rs

A. Sellinger · E. Leveugle · J.M. Fitz-Gerald · L.V. Zhigilei (✉)
Department of Materials Science and Engineering, University of Virginia, 395 McCormick Road, Charlottesville, VA 22904-4745, USA
e-mail: lz2n@virginia.edu

1 Introduction

The results of recent computational investigations of the mechanisms of molecular ejection and transport in the Matrix-Assisted Pulsed Laser Evaporation (MAPLE) thin film deposition technique have revealed that polymer molecules in MAPLE are ejected as parts of matrix-polymer clusters with a broad cluster size distribution [1–3]. The ejection of molecular clusters and droplets is inherently connected to the physical mechanism responsible for molecular ejection in MAPLE—explosive decomposition of a surface region of the target overheated up to the limit of its thermodynamic stability. The molecular-level simulations predict that material decomposition proceeds through the formation of a foamy transient structure of interconnected liquid regions that subsequently decomposes into a mixture of liquid droplets and gas-phase matrix molecules [1, 4]. Smaller clusters tend to originate from the front part of the emerging ablation plume whereas larger droplets lag behind and tend to have smaller ejection velocities, but both small and large clusters are unavoidable products of the collective material ejection process (ablation).

Although the results of the simulations dispute the original notion of the ejection and transport of individual polymer molecules in MAPLE [5–7], they provide an explanation for the significant surface roughness often observed upon close examination of the deposited films [8–14]. Moreover, the unusual wrinkled "deflated balloon" surface features, observed in recent MAPLE experiments [12, 14], can also be explained based on the ejection of large matrix-polymer droplets predicted in the simulations [1]. It has been demonstrated in a series of molecular dynamics (MD) simulations [15] that an internal release of the matrix vapor in a large matrix-polymer droplet is capable of pushing the polymer molecules to the outskirts of the droplet, thus forming

a transient "molecular balloon" expanding under the action of the internal vapor pressure. Active evaporation of matrix molecules from the surface of the droplet contributes to the formation of a polymer-rich surface layer, hampering the escape of the remaining matrix molecules. One can expect that following the deposition of a "molecular balloon" to a room-temperature substrate, the volatile matrix material enclosed by a polymer-rich layer would expand in time, resulting in the formation of release passages through the polymer layer, leaving behind characteristic wrinkled polymer structures, similar to those observed in experiments [2, 12, 14, 15].

In this paper, we report the results obtained by extending the initial computational work reported in [15] to simulations addressing questions on (1) the effect of the rate of the laser energy deposition on the formation and stability of the "molecular balloons" and (2) the relationship between the droplet landing velocity and the shapes of the polymer features observed on the surface. A brief description of the computational model used in the simulations is given in Sect. 2, followed by the presentation of results in Sects. 3 and 4. Based on computational predictions, an interpretation of several distinct types of surface features observed in MAPLE deposited films is provided in Sect. 5.

2 Computational model

A coarse-grained MD model, combining the breathing sphere model [16, 17] for simulation of the molecular matrix and the bead-and-spring model [18] for representation of polymer molecules, is used in the simulations. Intermolecular (nonchemical) interactions among the matrix and polymer molecules are described by an interatomic potential chosen to reproduce the van der Waals interactions in a typical molecular solid. In the bead-and-spring model, the "beads" representing functional groups of a polymer molecule (monomers) are connected by anharmonic springs with strengths appropriate for a carbon–carbon bond in a polymer molecule. Each monomer unit in a polymer molecule has the same molecular weight as a single matrix molecule, 100 amu. This weight corresponds to the weight of a PMMA monomer and is close to the weight of molecules typically used as MAPLE matrices, e.g., toluene (92 Da), chloroform (118 Da), and glycerol (92 Da). Each polymer chain contains 50 monomer units and has a total molecular weight of 5 kDa. A detailed description of the model, as well as the functional form and the parameters of the interaction potentials describing the intermolecular interactions and the chemical bonding in the polymer chains are given in [1].

3 Contribution of photomechanical effects to the formation of "molecular balloons"

Recent MD simulations of the response of matrix-polymer droplets to slow heating revealed an interesting effect of an internal release of matrix vapor leading to the spatial segregation of polymer and matrix molecules into a polymer-rich shell enclosing the volatile matrix molecules [15]. The formation of such balloon-like structures is predicted to occur as soon as the amount of the deposited thermal energy is sufficiently high for the droplet to exceed the threshold temperature T^* for the onset of a homogeneous explosive boiling or "phase explosion".[1] In particular, for droplets with initial polymer concentration of 16 wt.%, the deposition of thermal energy equal to 70% and 80% of the cohesive energy of the matrix material, E_c, resulted in heating in excess of T^*, Fig. 1a, triggering a rapid generation of matrix vapor inside the superheated droplet and leading to droplet disintegration at $0.8E_c$ and the formation of a "molecular balloon" at $0.7E_c$. At a lower energy density of $0.6E_c$, however, the maximum temperature barely reaches T^* by the end of the heating process and no internal boiling and associated molecular redistribution into a balloon-like structure is observed [15].

In the simulations reported in [15] and briefly described above, the rate of the energy deposition was sufficiently low to allow for the mechanical relaxation (expansion) of the droplets during the heating process. The characteristic time of the mechanical relaxation of a droplet with radius L can be estimated as $\tau_s \sim L/C_s$, where C_s is the speed of sound in the droplet material. Considering MAPLE experiments [3, 12, 14, 15] performed for toluene matrix ($C_s = 1306$ m/s [22]), the characteristic time of the mechanical relaxation of a toluene droplet with a radius on the order of micrometers is shorter than the experimental laser pulse duration of 25 ns. Although the exact heating regime experienced by droplets ejected in MAPLE experiments are not clearly established yet, one can expect that the droplets emerge in the overheated state from the explosive boiling of the irradiated target [1, 4] and, at laser fluences significantly exceeding the ablation threshold, can be further heated by the tail of the laser pulse. In any case, the heating time of the droplets is on the order of the laser pulse duration. Therefore, the experiments and simulations reported in [15] are performed

[1] A sharp transition from a metastable superheated liquid to a two-phase mixture of liquid and vapor at a temperature of approximately 90% of the critical temperature has been predicted based on the classical nucleation theory [19, 20] and confirmed in simulations [21]. The threshold temperature T^* is determined in a series of constant temperature and pressure MD simulations performed for a polymer-matrix system consisting of 134 000 matrix molecules and having a polymer concentration of 16 wt.%. The threshold temperature T^* corresponds to the onset of the phase separation and sharp increase of the volume of the system.

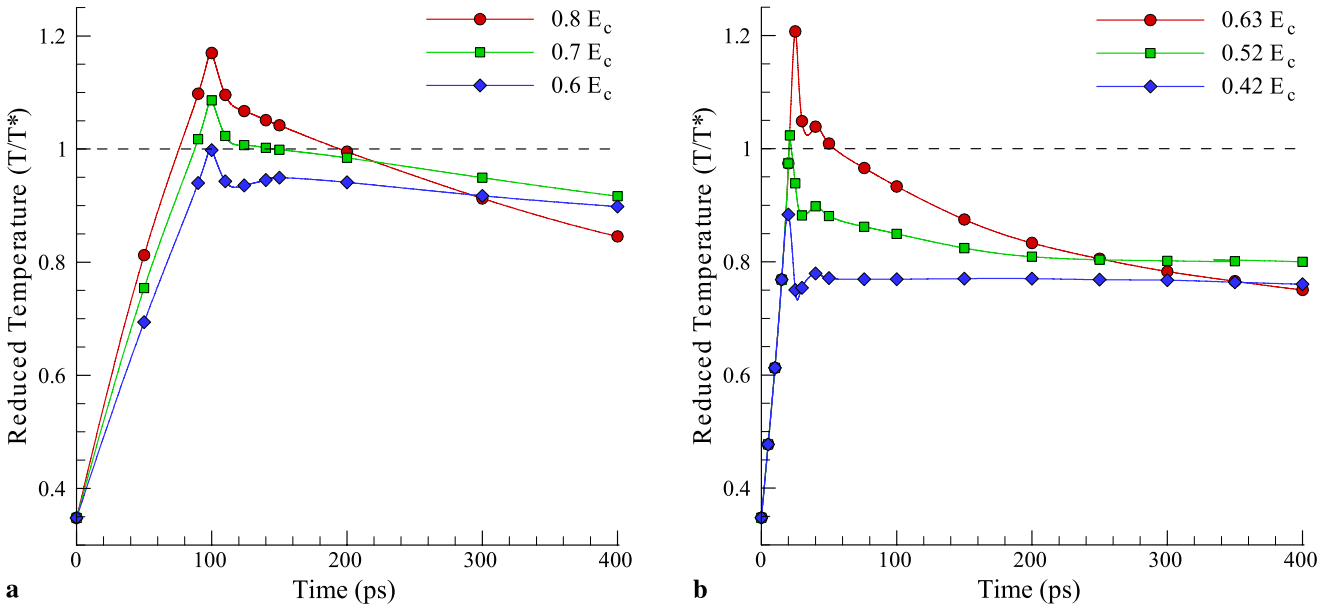

Fig. 1 Evolution of temperature during the first 400 ps of MD simulations of droplets heated during the first 100 ps (**a**) and 20 ps (**b**) of the simulations. The total amounts of the deposited energy correspond to 80, 70, and 60% (**a**) and 63, 52, and 42% (**b**) of the cohesive energy of the matrix material, E_c. Only the molecules that belong to the continuous droplets are included in the evaluation of the average temperature. The temperature values are normalized to the threshold temperature for the phase explosion, T^* (see footnote 1). Simulations performed with the slow energy deposition (**a**) are discussed in more detail in [15]. Snapshots from the simulations performed with the fast energy deposition (**b**) are shown in Fig. 2

under heating conditions that eliminate any significant contribution of photomechanical effects to the formation of the "molecular balloons."

In this work, we investigate the effect of the heating rate (related to the laser pulse duration in MAPLE experiments) on the behavior of the matrix-polymer droplets. Similar to [15], simulations are performed for droplets with an initial diameter of 60 nm and polymer concentration of 16 wt.%, but with a 5 times faster rate of energy deposition. In this case, the simulation conditions correspond to partial inertial stress confinement [17, 23, 24], the conditions under which compressive stresses build up during the heating process and photomechanical effects associated with the relaxation of the laser-induced stresses play an important role in defining the droplet behavior. The conditions of the inertial stress confinement can be realized in laser ablation experiments performed with shorter laser pulses or in two-pulse experiments where the second short pulse irradiation is used to modify the characteristics of the ablation plume.

Visually, the snapshots from the simulations, shown in Fig. 2, are similar to the ones observed with slower heating, although significantly lower energy densities are needed to achieve similar levels of droplet expansion. In particular, disintegration of the droplet into matrix vapor and polymer-rich fragments takes place at $0.63E_c$, Fig. 2a, whereas similar processes have been observed in the case of the slower heating at $0.8E_c$ [15]. The expansion of the droplets, observed at $0.52E_c$ (Fig. 2b) and $0.42E_c$ (Fig. 2c), does not result in disintegration but leads to the formation of transient spherical liquid shells encasing the volatile matrix vapor. By the time of the maximum expansion, ~200 ps, the shells attain a form resembling a gas-filled balloon. In both simulations, at $0.52E_c$ and $0.42E_c$, the shells, reinforced by continuous networks of entangled polymer chains, retain their integrity and remain hole-free. The expansion of the droplets is followed by contraction down to sizes similar to the original size before the beginning of the heating process. The final distribution of the polymer molecules within the droplets, however, is different from the original random arrangement, with the polymer molecules forming a polymer-rich shell around the volatile matrix trapped in the central part of the droplet, Figs. 2b and 2c. In particular, in the simulation performed at a deposited energy of $0.52E_c$, the evaporation of matrix molecules from the surface of the droplet results in an increase of the average polymer concentration in the droplet up to 20 wt.% by 1 ns, whereas the maximum polymer concentration in the polymer shell is approaching 39 wt.% by this time, more than twice the concentration in the original droplet. With a slower heating rate, outside the condition of stress confinement, similar molecular rearrangements leading to the formation of a polymer-rich shell enclosing matrix material has been observed in [15] at a significantly higher level of thermal energy deposition, $0.7E_c$. In both series of simulations, the evaporation of

matrix molecules diffusing through the polymer-rich shell continues throughout the duration of the simulation and results in a gradual cooling of the droplets and stabilization of the matrix core- polymer shell balloon-like structure of the droplet.

The effect of the rate of the energy deposition is apparent from comparison of the temperature plots shown for the two series of simulations in Fig. 1. For comparable energy depositions, the initial temperature increase is lower in the case of the slower heating, reflecting the cooling effect of the thermal expansion of the droplet during the heating process. In the simulations performed with the fast energy deposition, the expansion is initiated during the heating process but is completed after the heating stops, leading to the sharp temperature drop within ~10 ps after the end of the energy deposition, Fig. 1b. The initial temperature drop is followed by a slight increase of the temperature associated with the elastic contraction of the droplets and then by a gradual cooling associated with matrix vaporization. The vaporization can proceed by both the evaporation from the surface of the droplet and the internal release of vapor through the homogeneous nucleation of vapor regions inside the droplet. In the simulations where disintegration of the droplet is observed, the temperature decrease is particularly fast and, by the time of 400 ps, the temperature of the droplet drops below those for droplets with lower energy deposition. More violent phase decomposition and rapid expansion of the vapor and liquid fragments provide the conditions for faster cooling as compared to the evaporation of matrix from the polymer-rich shells enclosing the hot vapor.

In simulations performed with the slow heating [15], the condition for the internal release of vapor leading to the generation of a transient balloon-like structure or disintegration of the droplet is found to be simply $T^{\max} > T^*$. Indeed, in the simulation performed at $0.6E_c$, $T^{\max} \approx T^*$, and the droplet retains its internal integrity during the simulation [15]. In the simulations performed with faster heating, under the conditions of partial stress confinement, however, the formation of internal vapor regions and associated molecular redistribution into a polymer-rich shell and a matrix core is observed at much smaller energy densities of $0.52E_c$ and $0.42E_c$, when the average temperature of the droplet exceeds the threshold temperature T^* only for a few picoseconds ($0.52E_c$) or remains significantly below T^* for the whole duration of the simulation ($0.42E_c$).

The formation of the transient balloon-like structures at lower energy densities in the case of the fast heating, Figs. 2b and 2c, can be attributed to the photomechanical effects associated with the relaxation of the laser-induced stresses. The heating taking place faster than the droplet's expansion results in the build up of thermoelastic compressive stresses in the particle. The relaxation of the compressive stresses drives an unloading tensile pressure wave that propagates from the surface, focuses in the center of the droplet, and aids the nucleation and initial growth of vapor regions, as well as the expansion/disintegration of the droplet [23, 25]. Thus, the tensile stresses generated in the regime of stress confinement induce the homogeneous nucleation and growth of vapor bubbles at thermal energy densities at which no homogeneous boiling takes place without the assistance of tensile stresses.

4 The effect of the droplet landing velocity on the surface structures

The formation of "molecular balloons" predicted in the simulations provides a clue for explaining unexpected "deflated balloon"-like polymer structures observed in films deposited by MAPLE [2, 12, 14, 15]. The structure of the polymer features in the films, however, is defined not only by the characteristics of the droplets generated by laser ablation of a MAPLE target but also by the fast processes occurring during and immediately after the collisions of the droplets with the substrate, as well as by slower thermally-activated changes in the surface morphology of the growing films. While the slow changes in surface morphology are largely defined by the substrate temperature [13] and material viscosity, the initial generation of the surface features is related to the dynamics of the droplet-substrate collision and depends on the droplet landing velocity. In order to clarify the connections between the droplet landing velocity and the shapes of the polymer features generated on the substrate, we perform a series of MD simulations of the collision of a polymer-matrix droplet with a substrate. The simulations are performed for a droplet with a polymer-rich shell and a matrix core, obtained by the end of a 2 ns simulation of molecular rearrangements induced by a slow heating of a polymer-matrix droplet with a total deposited thermal energy of $0.7E_c$ [15]. The structure of the droplet is similar to the one shown for 1 ns in Fig. 2b. The strength of the interaction between the molecules and the substrate is set to be equal to that of molecule-molecule interactions. The simulations are performed for droplets impacting a rigid substrate with incident velocities of 100, 500, and 1000 m/s. These velocities are within the range predicted in large-scale MD simulations of MAPLE for clusters/droplets containing polymer molecules [1]. Similarly, nonthermal highly forward-peaked ejection velocities, with axial components ranging from hundreds to more than 1000 m/s have been measured for biomolecules of different masses, up to ~30 000 Da, in matrix-assisted laser desorption experiments [26–28]. The axial velocities of molecules and clusters are largely defined by the collective ejection process driven by the explosive decomposition of the overheated matrix and have a weak mass dependence [26, 27, 29].

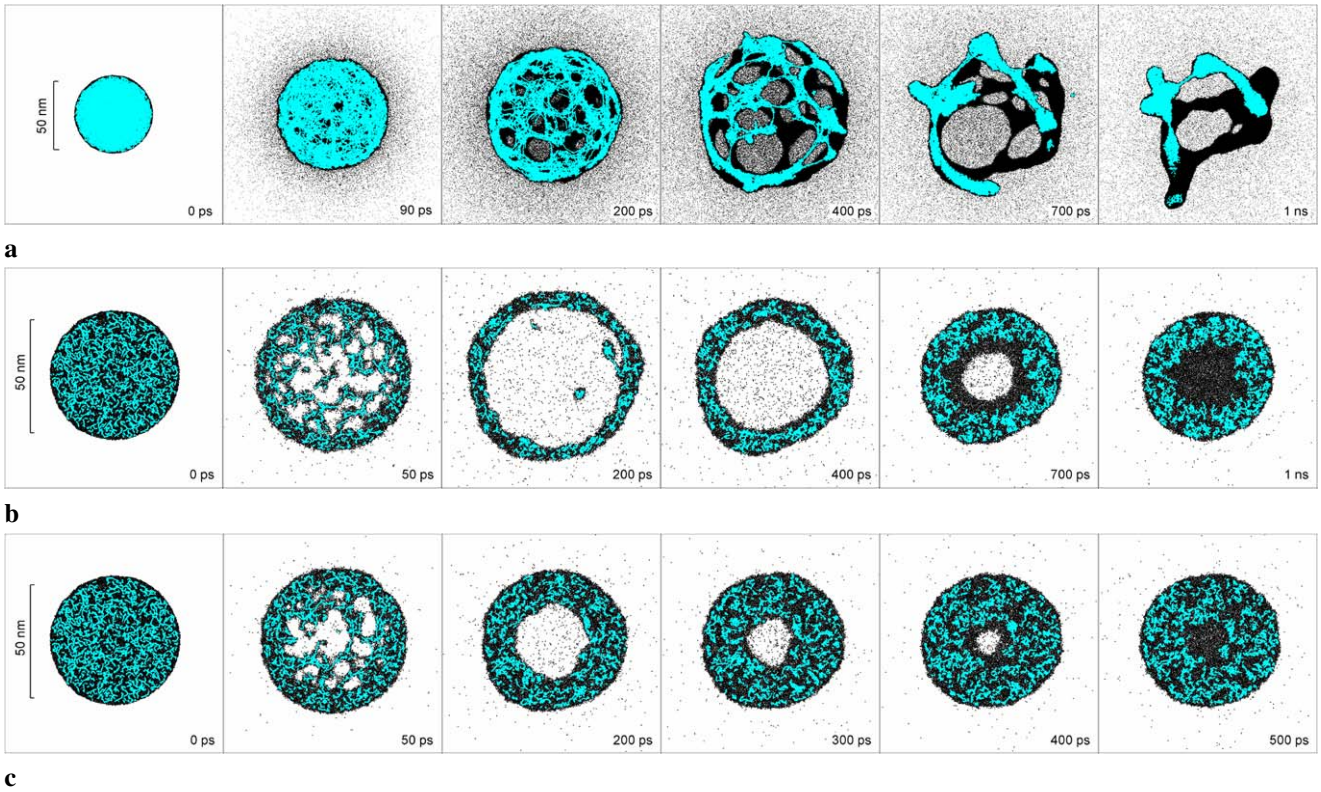

Fig. 2 Snapshots from MD simulations of the response of a 60 nm droplet to the fast energy deposition (regime of partial stress confinement). Droplets containing 16 wt.% of randomly oriented polymer chains are heated during the first 20 ps of the simulation, with the total amount of the deposited thermal energy equal to (**a**) 63%, (**b**) 52%, and (**c**) 42% of the cohesive energy of the matrix material, E_c. Matrix molecules and units of polymer chains are shown by *black* and *blue dots*, respectively. Polymer molecules in the front half of the computational cell are superimposed on top of the matrix molecules. Only 2 nm slices cut through the center of the droplet are shown in (**b**) and (**c**) to highlight the bulging of the cluster and segregation of the polymer molecules in the surface layer of the droplet. Animated sequences of snapshots from simulations illustrated in (**a**) and (**b**) can be found at http://www.faculty.virginia.edu/CompMat/molecular-balloons/

Snapshots from the simulations, shown in Fig. 3, provide a visual picture of the impact velocity dependence of the droplet-substrate collision dynamics. At 100 m/s, the droplet does not lose its integrity upon landing on the substrate, Fig. 3a. The impact results in a shape oscillation that quickly decays as the impact energy dissipates into heat. The characteristic molecular distribution in the original droplet (polymer-rich shell enclosing the matrix molecules) is retained in the deposited droplet, as can be seen from the snapshot shown in Fig. 3a for the time of 1 ns. This observation supports the explanation of the origin of the "deflated balloon" surface structures suggested in [15] and briefly outlined in the Introduction.

At higher deposition velocities of 500 and 1000 m/s, the impact energy is efficiently transferred to the energy of the material expansion in the lateral directions, leading to disintegration of the droplets. The impact also results in fast heating of the droplet, followed by fast cooling associated with transfer of the thermal kinetic energy into the energy of droplet disintegration, the energy of vaporization of a large fraction of the matrix content of the droplet, and the energy of the radial expansion of the droplet fragments.

The impact-induced heating and cooling due to the vaporization/disintegration are apparent from Fig. 4, showing the evolution of the temperature and concentration of the droplet and droplet fragments. The temperature is defined through the tangential component of the molecular velocities in cylindrical coordinates. Although the collision of a droplet with a substrate brings the system far from equilibrium, the tangential component of the molecular velocities does not have contributions from the initial motion of the droplet in the direction normal to the substrate, nor from the velocities arising from radial (along the substrate) expansion of the products of droplet disintegration. An average kinetic energy associated with the tangential velocity components, therefore, can be used as a rough measure of the amount of energy transferred to the increase of "temperature" of the droplet material, $T = 1/Nk_B \sum_N M v_t^2$, where v_t and M are the tangential velocity component and the mass of a molecule, respectively, k_B is the Boltzmann constant, and the summation is over N molecules that belong to the orig-

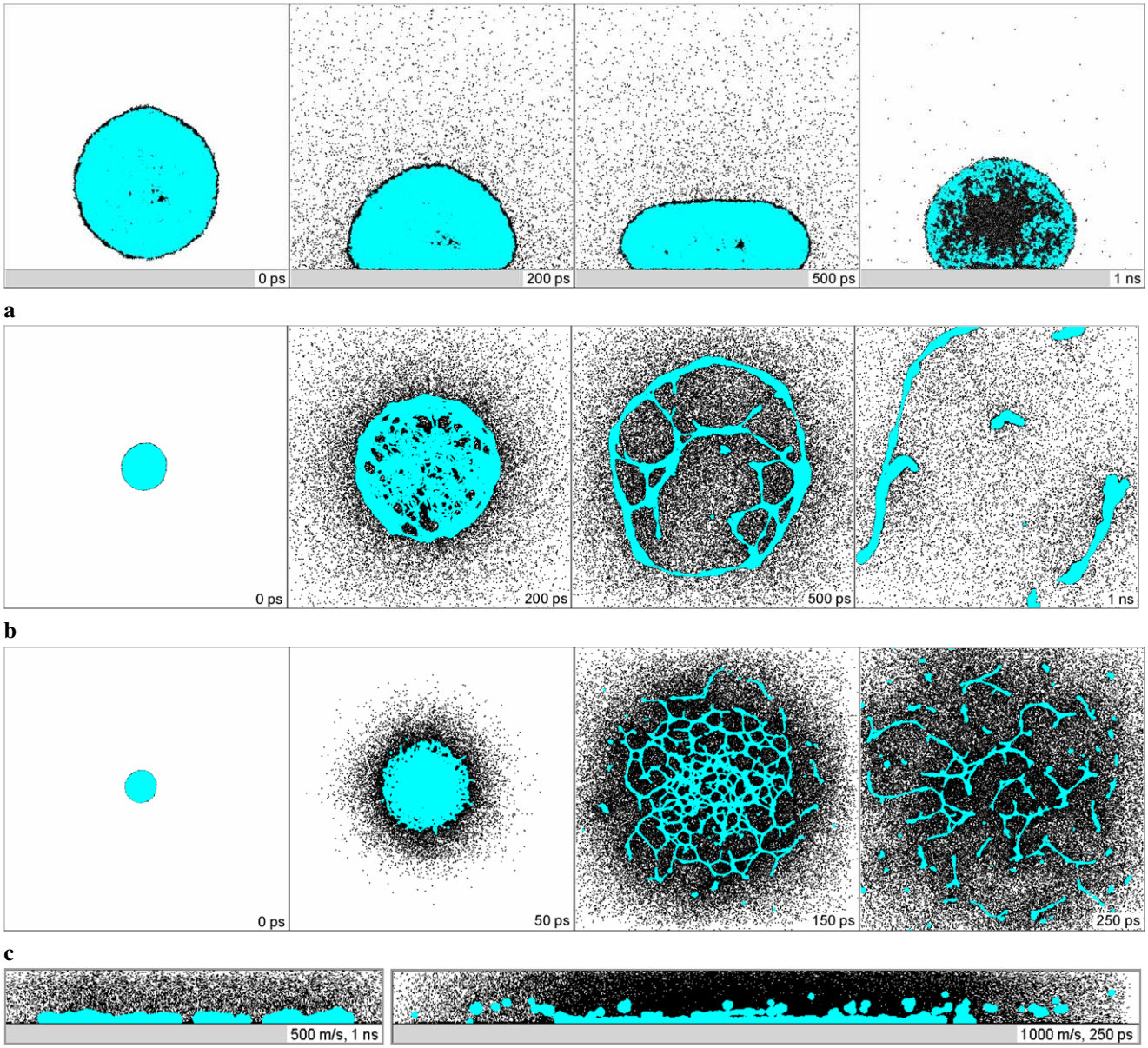

Fig. 3 Snapshots from MD simulations of the collision of a polymer-matrix droplet with a substrate performed for impact velocities of 100 m/s (**a**), 500 m/s (**b**), and 1000 m/s (**c**). Side view (parallel to the substrate) is shown in (**a**) and top view (along the impact direction) is shown in (**b**) and (**c**). Two additional snapshots providing side views of the final configurations obtained by the end of the simulations performed for 500 m/s (*left frame*) and 1000 m/s (*right frame*) are given in (**d**). The simulations are performed for a droplet with a polymer-rich shell and matrix core, obtained from a simulation reported in [15]. Matrix molecules and units of polymer chains are shown by *black* and *blue dots*, respectively. Polymer molecules in the front half of the computational cell are superimposed on top of the matrix molecules. Only a 2 nm slice cut through the center of the droplet is shown in the last snapshot in (**a**) to highlight the segregation of the polymer molecules in the surface layer of the droplet

inal continuous droplet or polymer-containing clusters that emerge from disintegration of the original droplet. The temperature spike is particularly sharp at the highest impact velocity of 1000 m/s, where the average temperature exceeds the threshold temperature for the phase explosion, leading to the rapid release of the matrix vapor and a violent droplet disintegration and expansion. The explosive decomposition of the overheated material is also reflected in the sharp increase of the polymer concentration in the remaining liquid fragments of the droplets, Fig. 4b. For the impact velocity of 100 m/s, the transfer of the impact energy to heat takes place over hundreds of picoseconds (Fig. 3a) and is offset by the

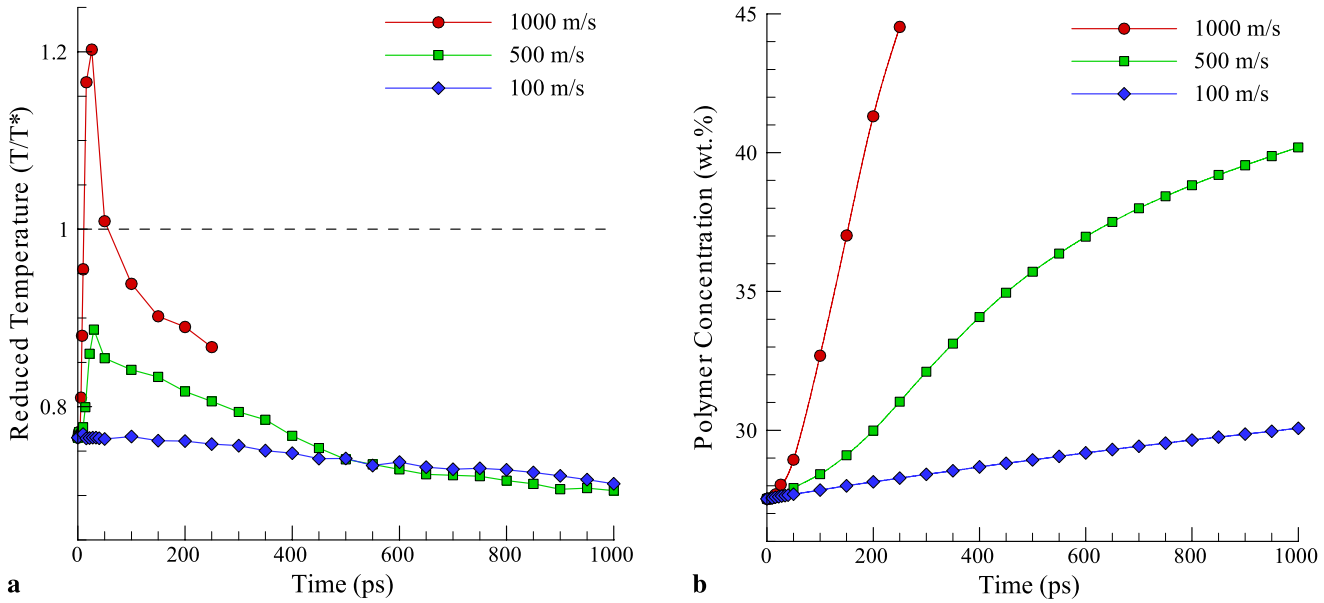

Fig. 4 Evolution of temperature and polymer concentration in MD simulations of the collision of a polymer-matrix droplet with a substrate performed for impact velocities of 100, 500, and 1000 m/s. The values of temperature and polymer concentration are calculated by averaging over molecules that belong to the original droplet or polymer-containing clusters that emerge from disintegration of the original droplet. The temperature is defined through the average kinetic energy associated with tangential velocity components of the matrix molecules and polymer units, as explained in the text. The temperature values are normalized to the threshold temperature for the phase explosion, T^* (see footnote 1). Snapshots from the simulations are shown in Fig. 3

gradual cooling due to continuous evaporation (Fig. 4b). As a result, no significant increase in the thermal energy is observed for this simulation in Fig. 4a.

The side-view snapshots from the simulations performed at deposition velocities of 500 and 1000 m/s, shown in Fig. 3d, demonstrate that the droplet fragments containing polymer molecules remain in close proximity to the substrate during the radial expansion. This enables additional cooling of the expanding fragments due to the heat transfer to the substrate, an effect that is not included in the present simulations. Although the radial expansion of the products of the droplet disintegration is not completed by the end of the simulations illustrated in Figs. 3b and 3c, one can expect that interaction with the substrate and cooling due to further matrix evaporation would eventually freeze and stabilize the polymer structures similar to the ones shown in the final snapshots taken in these simulations. In the next section, therefore, we compare the characteristic shapes of the droplet fragments observed in the simulations to the results of high-resolution scanning electron microscopy (SEM) imaging of films deposited in MAPLE experiments.

5 Connections to surface morphology in MAPLE experiments

Different types of polymer structures predicted in the simulations of the collision of a polymer-matrix droplet with a substrate can be related to SEM images of polymer films deposited by MAPLE. The images shown in Fig. 5 are taken from films deposited from a target containing 5 wt.% of poly(methyl methacrylate) (PMMA) dissolved in a toluene matrix. The depositions are performed at laser fluences of 500 mJ/cm^2 (a, c) and 300 mJ/cm^2 (b) with an excimer laser operating at a wavelength of 248 nm, pulse duration of 25 ns full width at half maximum, and pulse repetition rate of 5 Hz.

Several types of polymer surface features characteristic of the surface morphology of the deposited films can be identified in the images. The wrinkled "deflated balloon" surface features, such as the one shown in Fig. 5a, have been explained based on simulation results predicting the formation of balloon-like structures with a polymer-rich shell and a matrix core as a result of an internal boiling in polymer-matrix droplets ejected in MAPLE [1, 15]. The results presented in Sect. 3 confirm this mechanism and indicate that, in the case of faster heating, the onset of the internal boiling can be facilitated by photomechanical effects associated with the relaxation of the laser-induced stresses generated under the conditions of partial stress confinement. The dynamic molecular rearrangement leading to the formation of "molecular balloons," thus, appears to be a general phenomenon that takes place at different rates of laser energy deposition. In the SEM image shown in Fig. 5a, the "deflated balloon" polymer structure was sectioned using a focused

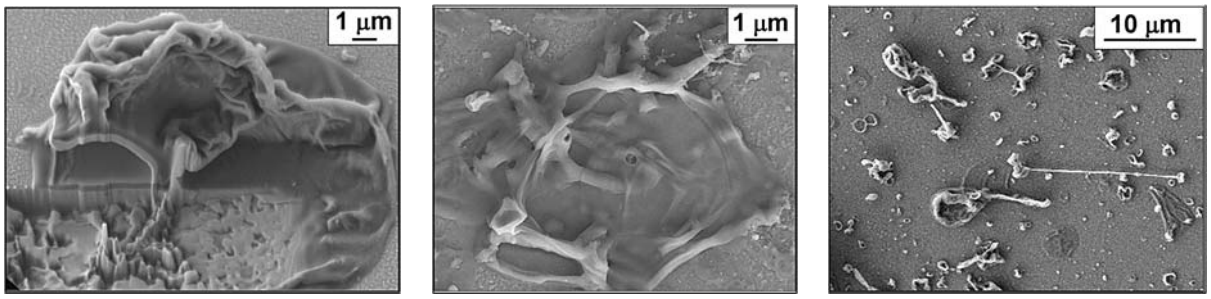

Fig. 5 SEM images of three characteristic surface features observed in MAPLE deposited thin films: (**a**) "deflated balloon," (**b**) localized network of interconnected polymer filaments, and (**c**) elongated "nanofibers." The images are taken from a film produced by MAPLE deposition from a target containing 5 wt.% of PMMA in a toluene matrix. The polymer structure in (**a**) is cut by a focused ion beam to expose the interior of the hollow structure

ion beam. Images were acquired off-axis with respect to the surface normal, providing a clear view of the hollow interior of the structure once occupied by the volatile matrix material.

Another distinct type of surface structure, a localized arrangement of interconnected polymer filaments, is illustrated in Fig. 5b. The structure of this polymer surface feature is similar to the intermediate structures observed in simulations where droplet disintegration takes place, e.g., 500 ps in Fig. 3b and 150 ps in Fig. 3c. Under conditions of sufficiently fast cooling enhanced by heat conduction to the substrate, such intermediate structures can be stabilized during the expansion, resulting in surface patterns similar to the ones observed in experiments.

The third type of surface feature commonly observed in SEM images of films deposited by MAPLE [2, 3, 12, 14] is an elongated "nanofiber," such as the one shown in Fig. 5c. The unusual elongated shapes of the deposited surface features have been related in [1] to the formation and ejection of long polymer-rich filaments observed in large-scale MD simulations of MAPLE. The ejection of the filaments is related to the entanglement of the polymer chains that becomes more pronounced with increasing polymer concentration in the target. The results of the simulations of droplet collisions with the substrate, discussed in Sect. 4, suggest an additional scenario for the formation of the elongated polymer structures. The elongated polymer "nanofibers" or "necklace" polymer surface features can be generated as a result of the expansion and freezing of the droplet disintegration products, similar to the ones shown in the last snapshot in Fig. 3b.

Although the MD simulations reported in this paper are aimed at revealing the mechanisms responsible for generation of surface features in films deposited in MAPLE, the results of the simulations may have implications for a broader range of target materials used in laser-assisted film deposition. Laser ablation of polymer targets, in particular, often involves photothermal and/or photochemical decomposition of the target material, with volatile species released in the photothermal/photochemical reactions playing a role in material ejection similar to that of the matrix in MAPLE. The results of the simulations performed for polymer-matrix droplets, therefore, can help in interpretation of the surface structures observed in films deposited by laser ablation of polymer targets, e.g., elongated surface features in films fabricated by IR laser ablation of poly(vinil chloride) [30].

Acknowledgements Financial support of this work is provided by the National Science Foundation through grants DMII-0422632 and NIRT-0403876. L.V.Z. gratefully acknowledges a travel grant to attend COLA'07 from DYNA program of the European Science Foundation.

References

1. E. Leveugle, L.V. Zhigilei, J. Appl. Phys. **102**, 074914 (2007)
2. E. Leveugle, L.V. Zhigilei, A. Sellinger, J.M. Fitz-Gerald, J. Phys.: Conf. Ser. **59**, 126 (2007)
3. E. Leveugle, L.V. Zhigilei, A. Sellinger, J.M. Fitz-Gerald, Appl. Surf. Sci. **253**, 6456 (2007)
4. L.V. Zhigilei, Appl. Phys. A **76**, 339 (2003)
5. A. Piqué, R.A. McGill, D.B. Chrisey, J. Callahan, T.E. Mlsna, Mat. Res. Soc. Symp. Proc. **526**, 375 (1998)
6. A. Piqué, R.A. McGill, D.B. Chrisey, D. Leonhardt, T.E. Mslna, B.J. Spargo, J.H. Callahan, R.W. Vachet, R. Chung, M.A. Bucaro, Thin Solid Films **355/356**, 536 (1999)
7. D.B. Chrisey, A. Piqué, R.A. McGill, J.S. Horwitz, B.R. Ringeisen, D.M. Bubb, P.K. Wu, Chem. Rev. **103**, 553 (2003)
8. A. Gutierrez-Llorente, R. Perez-Casero, B. Pajot, J. Roussel, R.M. Defourneau, D. Defourneau, J.L. Fave, E. Millon, J. Perriere, Appl. Phys. A **77**, 785 (2003)
9. R. Cristescu, D. Mihaiescu, G. Socol, I. Stamatin, I.N. Mihailescu, D.B. Chrisey, Appl. Phys. A **79**, 1023 (2004)
10. A.L. Mercado, C.E. Allmond, J.G. Hoekstra, J.M. Fitz-Gerald, Appl. Phys. A **81**, 591 (2005)
11. R. Fryček, M. Jelínek, T. Kocourek, P. Fitl, M. Vrňata, V. Myslík, M. Vrbová, Thin Solid Films **495**, 308 (2006)
12. A.T. Sellinger, E.M. Leveugle, K. Gogick, L.V. Zhigilei, J.M. Fitz-Gerald, J. Vac. Sci. Technol. A **24**, 1618 (2006)

13. K. Rodrigo, P. Czuba, B. Toftmann, J. Schou, R. Pedrys, Appl. Surf. Sci. **252**, 4824 (2006)
14. A.T. Sellinger, E. Leveugle, K. Gogick, G. Peman, L.V. Zhigilei, J.M. Fitz-Gerald, J. Phys.: Conf. Ser. **59**, 314 (2007)
15. E. Leveugle, A. Sellinger, J.M. Fitz-Gerald, L.V. Zhigilei, Phys. Rev. Lett. **98**, 216101 (2007)
16. L.V. Zhigilei, P.B.S. Kodali, B.J. Garrison, J. Phys. Chem. B **101**, 2028 (1997)
17. L.V. Zhigilei, E. Leveugle, B.J. Garrison, Y.G. Yingling, M.I. Zeifman, Chem. Rev. **103**, 321 (2003)
18. *Computer Simulation of Polymers*, ed. by E.A. Colbourn (Longman Scientific and Technical, Harlow, 1994)
19. A. Miotello, R. Kelly, Appl. Phys. A **69**, S67 (1999)
20. N.M. Bulgakova, I.M. Bourakov, Appl. Surf. Sci. **197**, 41 (2002)
21. B.J. Garrison, T.E. Itina, L.V. Zhigilei, Phys. Rev. E **68**, 041501 (2003)
22. *Kaye and Laby Online Tables of Physical and Chemical Constants* (National Physical Laboratory, Teddington, 2007). http://www.kayelaby.npl.co.uk/
23. G. Paltauf, P.E. Dyer, Chem. Rev. **103**, 487 (2003)
24. E. Leveugle, D.S. Ivanov, L.V. Zhigilei, Appl. Phys. A **79**, 1643 (2004)
25. L.V. Zhigilei, B.J. Garrison, Appl. Surf. Sci. **127–129**, 142 (1998)
26. R.C. Beavis, B.T. Chait, Chem. Phys. Lett. **181**, 479 (1991)
27. Y. Pan, R.J. Cotter, Org. Mass Spectrom. **27**, 3 (1992)
28. A.A. Puretzky, D.B. Geohegan, G.B. Hurst, M.V. Buchanan, B.S. Luk'yanchuk, Phys. Rev. Lett. **83**, 444 (1999)
29. L.V. Zhigilei, B.J. Garrison, Rapid Commun. Mass Spectrom. **12**, 1273 (1998)
30. J. Blazevska-Gilev, J. Kupčík, J. Šubrt, Z. Bastl, V. Vorlíček, A. Galíková, D. Spaseska, J. Pola, Polym. Degrad. Stab. **91**, 213 (2006)